FUNCTION american physiological society

FUNCTION, 2025, 6(2): zqaf014

https://doi.org/10.1093/function/zqaf014
Advance Access Publication Date: 5 March 2025
Original Research

ORIGINAL RESEARCH

High-Salt Diet Increases Suprachiasmatic Neuronal Excitability Through Endothelin Receptor Type B Signaling

Jodi R. Paul[1], Megan K. Rhoads[2], Anna Elam[1], David M. Pollock[2,*], Karen L. Gamble[1,*]

[1]Division of Behavioral Neurobiology, Department of Psychiatry, University of Alabama at Birmingham, Birmingham, Alabama, 35294, USA, [2]Section of Cardio-Renal Physiology and Medicine, Division of Nephrology, Department of Medicine, University of Alabama at Birmingham, Birmingham, Alabama, 35233, USA

*Address correspondence to K.L.G. (e-mail: klgamble@uab.edu), D.M.P. (e-mail: davidpollock@uabmc.edu)

Abstract

Circadian rhythms are 24-h oscillations in behavioral and biological processes such as blood pressure and sodium excretion. Endothelin B (ET_B) receptor has been connected to the molecular clock in peripheral tissues and plays a key role in the regulation of sodium excretion, especially in response to a high-salt diet. However, little is known about the role of ET_B in the primary circadian pacemaker in the brain, the suprachiasmatic nucleus (SCN), despite recent reports showing its enrichment in SCN astrocytes. In this study, we tested the hypothesis that high-salt diet (4.0% NaCl) impacts the circadian system via the ET_B receptor at the behavioral, molecular, and physiological levels in C57BL/6 mice. Two weeks of high-salt diet feeding changed the organization of nighttime wheel-running activity, as well as increased the SCN expression of ET_B mRNA determined by fluorescence in situ hybridization at night. Neuronal excitability determined using loose-patch electrophysiology was also elevated at night. This high-salt diet-induced increase in SCN activity was ameliorated by ex vivo bath application of an ET_B antagonist and could be mimicked with acute treatment of endothelin-3. Finally, we found that the excitatory effects of endothelin-3 were blocked with co-application of an N-methyl-D-aspartate (NMDA) receptor antagonist, suggesting that glutamate mediates endothelin-induced neuronal excitability in the SCN. Together, our data demonstrate the presence of functional ET_B receptors in SCN astrocytes and point to a novel role for endothelin signaling in mediating neuronal responses to a dietary sodium intake.

Submitted: 24 December 2024; **Revised:** 12 February 2025; **Accepted:** 2 March 2025

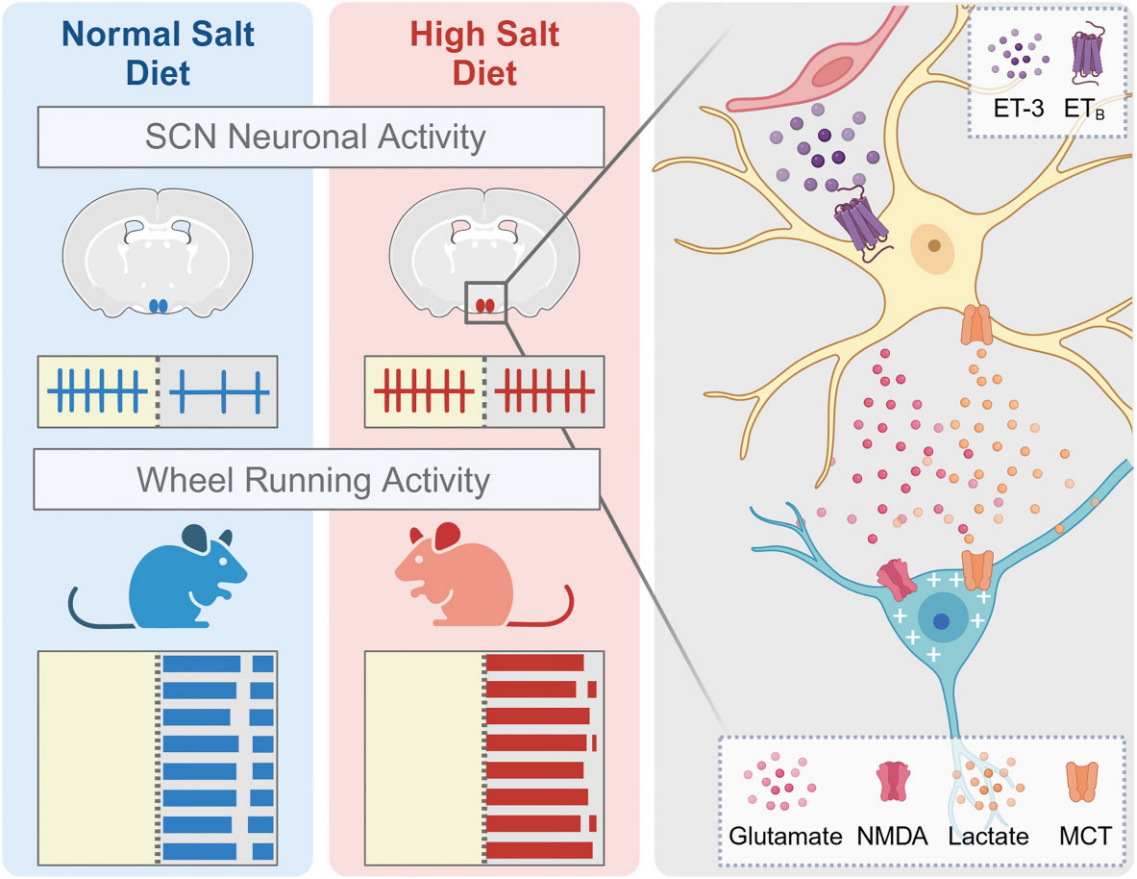

Key words: circadian behavior; endothelin; sodium; neurophysiology; astrocytes; electrophysiology

Introduction

Circadian rhythms are 24-h oscillations in behavioral and physiological processes such as blood pressure and sodium excretion.[1,2] At the cellular level, circadian rhythms are controlled by a transcriptional translational feedback loop of core clock genes, which drive time-of-day changes in expression of numerous, tissue-specific, clock-controlled genes.[3] While these local circadian "clocks" exist throughout all tissues, the central pacemaker—the suprachiasmatic nucleus (SCN) of the hypothalamus—serves as the primary clock for the body. The SCN is responsible for synchronizing peripheral tissues and the rhythms they drive with external time cues such as light as well as other secondary clocks. Time-of-day information is communicated by the SCN to local clocks through daily rhythms in spontaneous neuronal activity, with high activity during the day and low activity at night.[4] Recent work has demonstrated that this canonical SCN output is affected by acute salt loading through signaling from the organum vasculosum of the lamina terminalis (OVLT),[5] yet the effect of chronic consumption of a high-salt diet (HSD) is still unknown. It is well known that homeostatic control of thirst and acute drinking behavior is driven by the subfornical organ (SFO), which induces a rapid increase in water intake in response to hyperosmolarity (for review see Zimmerman[6]). However, the recent emergence of the SCN-OVLT axis as a driver of daily rhythms in fluid intake, independent of plasma osmolarity,[5,7] has highlighted the SCN response to HSD as a remaining gap in our current understanding.

The endothelin system plays an important role in cardiovascular regulation and fluid-electrolyte homeostasis.[8] This system is made up of 2 G-protein–coupled receptors and 3 structurally similar ligands,[8] with many of these components present in the hypothalamus.[9] Endothelin B (ET_B) receptors in the kidney play a key role in the excretion of salt and regulation of blood pressure, particularly in response to an HSD.[10] Specifically, endothelin-1 (ET-1) functions as an autocrine factor to stimulate ET_B receptors in response to an HSD to inhibit the reabsorption of sodium. Loss of ETB receptor function impairs the ability of the kidney to excrete salt and so the resulting salt-dependent hypertension is necessary for maintaining balance between intake and excretion.[9] Recent evidence from our group and others suggests a connection between the molecular clock and the endothelin system in peripheral tissues.[2,11] Interestingly, single-cell RNA sequencing of the SCN has revealed that *Ednrb* encoding ET_B is expressed in SCN astrocytes. Moreover, SCN endothelial cells rhythmically express clock genes as well as *Edn3* (encoding endothelin-3 or ET-3).[12] This result suggests that the endothelin system has a physiological role in the SCN, and although several studies have examined endothelin in other hypothalamic nuclei,[13,14] the functional role of the endothelin system in the SCN remains unexplored. Therefore, the goal of this study was to determine the potential role for ET_B in the SCN, and specifically, the SCN response to an HSD.

Materials and Methods

Animals

Male and female, 2-month-old C57BL6/J mice were bred in house or purchased from Jax (Strain #:000664) and then group housed (unless otherwise noted) in a 12:12 light/dark (LD) cycle with food and water provided ad libitum. For the day/night and pharmacological recordings, mice were acclimated to a reverse LD cycle ≥2 weeks before feeding interventions. Mice were fed either an HSD (4% NaCl, Teklad Diets, #92034) or normal salt diet (NSD, 0.49% NaCl) for 2 weeks prior to experiments and were euthanized with cervical dislocation and rapid decapitation. The 2-week period was chosen to allow animals to adjust the many factors that regulate fluid electrolyte balance and is typical of that used in rodent studies.[15–18] All animal procedures were approved by the University of Alabama at Birmingham Institutional Animal Care and Use Committee in accordance with the NIH *Guide for the Care and Use of Laboratory Animals*.

Behavior

To avoid the confounding effects of the estrous cycle on wheel-running activity such as an inconsistent "siesta" period,[19,20] only male mice were used for this experiment. Male mice aged 3-4 months were single-housed in individual wheel-running cages, and wheel-running activity was recorded and analyzed with ClockLab software (Actimetrics, Wilmette, IL). Mice assigned to the HSD group were switched to HSD when first placed in wheel-running cages, while NSD mice continued on normal chow. Behavior was analyzed across days 11-19 after start of diet to allow time for acclimation to wheel-running cages. Actograms of activity in 6-min bins were used to determine the time of activity onset and offset as well as alpha length as previously described.[21] Average activity profiles in 1-h bins were used to compare activity between groups across full 24-h cycle. Individual activity profiles in 30-min bins were used to determine time of "siesta" and length of the first and second bouts of activity per night. Time of "siesta" was defined as the 30-min period of lowest activity between Zeitgeber time (ZT) 18-23 (where ZT 12 refers to lights off).[22] The start and the end of each activity bout were determined as the first 30-min bin that crossed above or below 50% maximum activity, respectively (see Figure 1C) and were used to calculate the first and second bout duration.[23] In mice without a second peak in activity or where the second peak did not cross this threshold, the second bout duration was considered zero.

Electrophysiology

Male and female mice were fed HSD or NSD for 2 weeks ad lib starting at 2.5 months of age. Fresh brain slices were prepared using previously published methods (as in Paul et al.[24]). Briefly, brains were submerged in ice-cold oxygenated sucrose saline (in mM): 250 sucrose, 26 $NaHCO_3$, 1.25 Na_2-HPO_4-$7H_2O$, 10 glucose, 2.5 $MgCl_2$, and 3.5 KCl, and coronal SCN–containing sections (200 μm) sections were taken on a vibroslicer (Campden 7000SMZ, World Precision Instruments). Slices were rested for ~20 min at RT in an oxygenated mixture of 50% sucrose saline and 50% extracellular solution (in mM): 130 NaCl, 20 $NaHCO_3$, 1 Na_2-HPO_4-$7H_2O$, 10 glucose, 1.3 $MgSO_4$-$7H_2O$, 3.5 KCl, and 2.5 $CaCl_2$. Slices were transferred to a heated (34°C ± 0.5°C) recording chamber and continuously perfused (2 mL/min) with oxygenated extracellular solution for the duration of the recording window. For pharmacological experiments, treatments were bath-applied 30 min before the start of recordings and remained in bath throughout the 4-h window. Individual cells were visualized using differential interference contrast (DIC) on an Axio Examiner microscope (Carl Zeiss Inc.). Targeted loose-patch recordings were made from SCN neurons during the day (ZT 4-8) or night (ZT 14-18) using 3-5 MΩ resistance glass pipettes filled with internal solution (in mM): 150 NaCl, 10 4-(2-hydroxyethyl) piperazine-1-ethanesulfonic acid (HEPES), 10 glucose, 2.5 $CaCl_2$, 1.3 $MgCl_2$, and 3.5 KCl. Electrophysiological recordings were sampled at 20 kHz and filtered at 10 kHz using a Multiclamp 700B amplifier and pClamp 11.2 software (Axon Instruments). Spontaneous firing rate was measured using 2-min recordings in gap-free mode and analyzed in Clampfit 11.2.

Pharmacology

IRL-1620 (Tocris, #1196), ET-3 (Tocris, #1162), and 3-(2-carboxypiperazin-4-yl)propyl-1-phosphonic acid (CPP, Abcam, ab144495) were dissolved in water. A-192621 (Med Chem Express, HY-120295) and 2-cyano-3-(4-hydroxyphenyl)-2-propenoic acid (CHC; Tocris, #5029) were dissolved in dimethyl Sulfoxide (DMSO) before being added to recording solution for a final working concentration of 0.03% and 0.2% DMSO, respectively.

Fluorescence in Situ Hybridization

Fresh frozen brain tissue was sectioned at 15-μm thickness through the SCN and mounted on glass slides. Slides were stored at −80°C until ready for staining. Sections were stained using the manufacturer-designed probes for *Ednrb* (Advanced Cell Diagnostics Bio catalog #473801), *Eno2* (catalog #517261), and *Gfap* (catalog #313211) according to the manufacturer's recommended protocols. Briefly, slides were fixed in 10% neutral buffered formalin at 4°C for 15 min. Slides were then dehydrated through an ethanol series, then dried at RT for 5 min. A hydrophobic barrier was drawn around the section and the tissue incubated with protease IV for 30 min at RT. After washing in phosphate buffered saline (PBS) , slides were incubated with the appropriate probe mix for 2 h at 40°C in the HybEZ II Oven (ACD Bio). Sections were then processed with the RNAScope Fluorescent Multiplex Assay v2 reagents using the manufacturer's recommendations.

Images were quantified using a custom semi-automated pipeline in Cell Profiler (v4.2.1). Briefly, DAPI was used to identify nuclei within the boundaries of the SCN, which were then used to identify *Ednrb*-positive nuclei. The region of interest (ROI) for *Ednrb*-positive nuclei was then expanded out by 10 pixels. *Ednrb* expression was measured as the percentage of an ROI area, which was covered by *Ednrb* signal.

Statistical Analysis

All data were analyzed using SPSS 29 (IBM). All data were tested for assumptions of normality and homogeneity of variances, and violations of these assumptions were handled with transformations or use of nonparametric tests as needed. Behavioral data were analyzed using independent-samples t-tests or 2-way, repeated-measures analysis of variance (ANOVA) with Holm-Bonferroni-corrected post hoc. Fluorescence in situ hybridization (FISH) data were square root-transformed to correct for a non-normal distribution and analyzed with a linear mixed model with a first-order auto-regressive covariance structure using "batch" as a covariate and "time" and "diet" as fixed factors and repeated measures across cells within each brain. Estimated marginal means (EMM) and 95% CI reported in results were

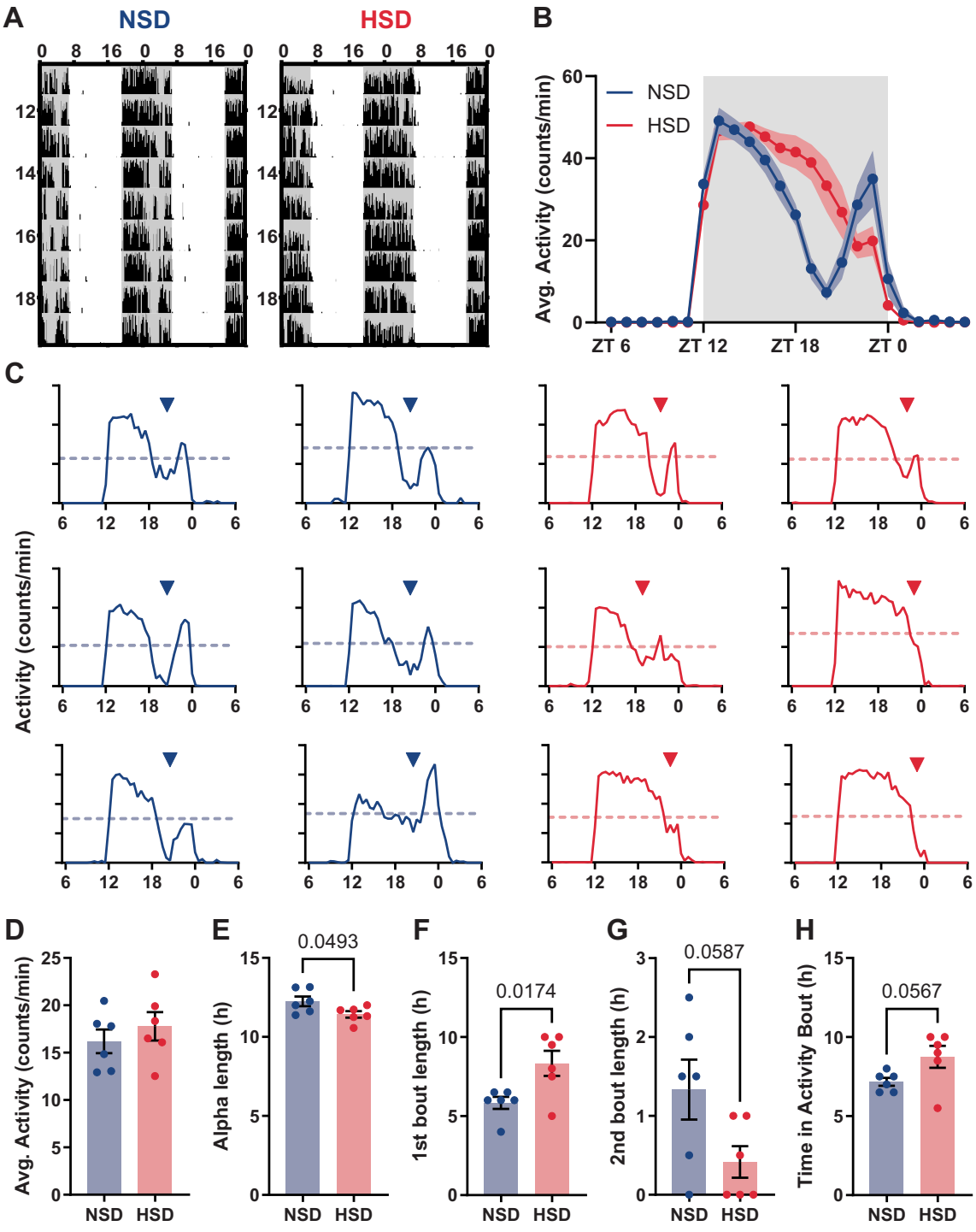

Figure 1. High-salt diet (HSD) alters the pattern of daily wheel-running activity. (A) Representative double-plotted actograms of wheel-running activity from mice fed normal salt diet (NSD) (left) or HSD (right) for 2 weeks prior to analysis. Periods of dark indicated by gray shading. (B) Means ± SEM of average 24-h activity profile for mice represented in A, plotted in 1-h bins revealed differences in organization of activity (time × diet interaction, $F_{(5.861, 58.61)} = 110.725$; $P < .001$). Specifically, HSD-fed mice had significantly higher activity at Zeitgeber time (ZT) 19 (Holm-Bonferroni post hoc, $P = .013$). (C) Activity profiles for individual NSD- (two left traces in each row) or HSD-fed (two right traces in each row) mice plotted in 30-min bins used for analysis of siesta period (triangle) and the first and second activity bouts (see methods). Dotted line indicates 50% max activity for each animal. (D-H) Means ± SEM for average activity (D; $t_{(10)} = 0.813$), alpha length (E; $t_{(10)} = -2.24$), length of first activity bout (F, $t_{(10)} = 2.845$), length of the second activity bout (G, $t_{(10)} = -2.133$), and total time in activity bout (*H*, $t_{(10)} = 2.154$). Dots represent values for individual animals. $N = 6$ mice per group.

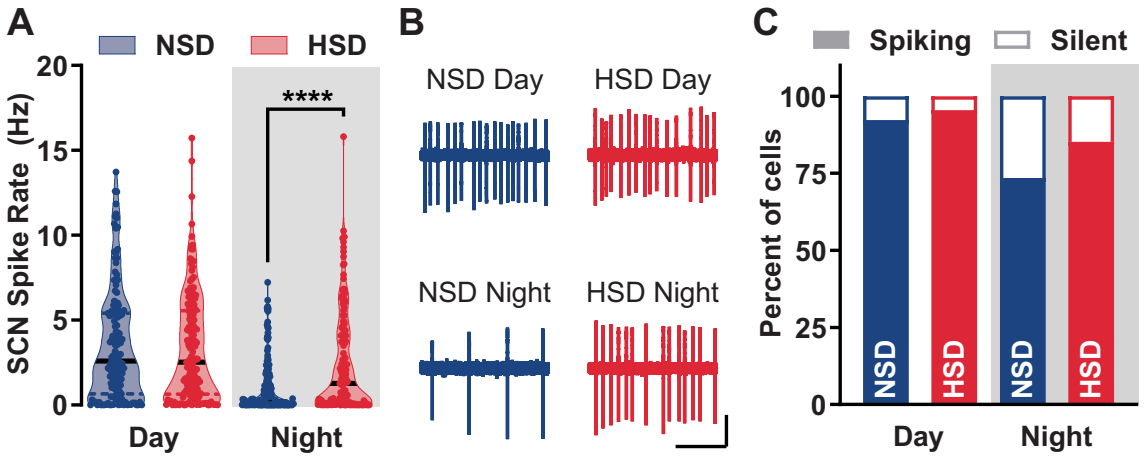

Figure 2. High-salt diet (HSD) increases suprachiasmatic nucleus (SCN) neuronal excitability at night. (A) Violin plots of spontaneous action potential frequencies of SCN neurons from mice fed normal salt diet (NSD) or HSD for 2 weeks, recorded during the day (Zeitgeber time [ZT] 4-8) or night (ZT 14-18). HSD significantly increased SCN firing at night (time × diet interaction, $H_{(1)} = 10.392$, $P = .001$; NSD-night vs. HSD-night post hoc, $P < .001$), but had no effect during the day ($P = 1.00$). Solid and dotted lines indicate median and quartiles, respectively. $n = 143$ (NSD-day), 155 (HSD-day), 151 (NSD-night), and 155 (HSD-night) cells; 4 mice per group. (B) Representative loose-patch traces (5 s) from each group. Scale bars: 2 s, 50pA. (C) Percentage of silent (empty bars) versus spiking (filled bars) cells for each group in A and B. Three-way loglinear analysis revealed a significant increase in silent cells at night for both diets (time × spiking interaction, $\chi^2_{(1)} = 28.949$, $P < .001$), as well as an increase in the proportion of spiking cells in HSD mice at both times of day (diet × spiking interaction, $\chi^2_{(1)} = 7.661$, $P = .006$).

back transformed for clarity of interpretation. Due to the non-normal distribution of SCN spike rate data, loose-patch results were analyzed with nonparametric Kruskal-Wallis tests (Figure 4) or the Scheirer-Ray-Hare extension of the Kruskal-Wallis tests, which allows for a 2 × 2 design. Sex was included as a factor in initial analysis of electrophysiological data and found to have no significant main effect or interactions; thus, data from male and females animals were combined for the final analysis. Contingency data were analyzed with 3-way loglinear analysis and χ^2 tests. Significance was ascribed at $P < .05$.

Results

To examine the impact of dietary salt intake on daily activity patterns, male C57 mice were placed in wheel-running cages and fed high (4% NaCl) or normal (0.49% NaCl) salt diet. Consistent with our previous work in rats,[25] HSD did not impact the overall activity levels in mice (Figure 1A and D). However, HSD changed the organization of activity across the 24-h cycle (Figure 1B). Specifically, HSD-fed animals had increased activity at ZT 19. Interestingly, this time of the night is typically referred to as the "siesta" period—the approximately 2-h period in the late night where mice will sleep.[22] In fact, when we examined the timing of the mid-point of the "siesta" period (as defined in the "Materials and Methods" section), HSD-fed mice trended toward a later siesta (mean ± SEM: HSD, 21.83 ± 0.62; t-test, $t_{(5)} = 2.169$, $P = .082$) but with significantly greater variability across animals; whereas in NSD-fed mice, the siesta mid-point occurred at ZT 20.5 for every mouse (Levene's test, $F_{(1,10)} = 7.191$, $P = .023$; Figure 1C arrowheads). Moreover, the first nightly bout of activity was >2 h longer in HSD-fed mice on average (Figure 1F), while there was a trend for the second, post-rest, bout of activity to be shorter in HSD-fed mice (Figure 1G). This change to the late-night rest period is was also reflected in the trend for HSD-fed mice to spend more time of the night in an activity bout (Figure 1H), despite significantly longer alpha lengths (time between activity onset and activity offset) of NSD-fed mice (Figure 1E). Together, these results suggest, HSD-fed mice are less likely to take a siesta, and if a siesta is present, it is likely to be shorter in duration.

We next sought to determine whether changes in SCN output could account for the HSD-induced changes in behavior. To do this we examined spontaneous action potential firing from SCN neurons during the day or night after 2 weeks on an HSD or NSD. As expected, NSD-fed mice had a day/night difference in SCN spike rate, with higher activity during the day (median [interquartile range or IQR]: NSD-day, 2.59 [0.65-5.40]; NSD-night, 0.19 [0.00-1.49 Hz]; Figure 2). This day/night difference was blunted in neurons from mice fed an HSD (median [IQR]: HSD-day, 2.52 [0.64-5.55]; HSD-night, 1.28 [0.07-4.07 Hz]). Interestingly, this change was specifically driven at night, at which time the average spike rate of neurons from HSD-fed mice was more than double that of NSD neurons. Additionally, HSD decreased the proportion of silent cells compared to NSD across both times of day, with HSD cells 2.07 times more likely to be spiking at night than NSD cells (Figure 2C).

Previous work has demonstrated that HSD increases the expression of components of the ET system in various extrarenal tissues including endothelial cells.[26–28] However, less is known about the impact of the ET system in the central regulation of acclimation to an HSD despite evidence for endothelial cell expression of *Edn3* in the SCN (Supplemental Figure S1; Wen et al.[12]), as well as expression of ET_B receptors in multiple hypothalamic regions, including the SCN.[9,12,29] To determine whether there is differential expression of *Ednrb*, the gene encoding ET_B receptors, about the day versus night or HSD versus NSD, we next used FISH to probe for *Ednrb* in SCN sections from NSD- and HSD-fed animals collected at ZT 6 (day) or ZT 18 (night). SCN cells exhibited a significant diurnal difference in *Ednrb* expression, with higher expression during the day (main effect of time, $F_{(1975)} = 4.779$, $P = .029$); however, this day/night difference was blunted in HSD-fed animals (Figure 3). Specifically, HSD significantly increased *Ednrb* expression by 1.26 fold compared to NSD at night (EMM [95% CI]: HSD-night, 24.9% [23.7-26.2]; NSD-night, 19.7% [18.4-21.1]) but did not have a significant effect on *Ednrb* expression during the day (EMM [95% CI]: HSD-day, 23.3%

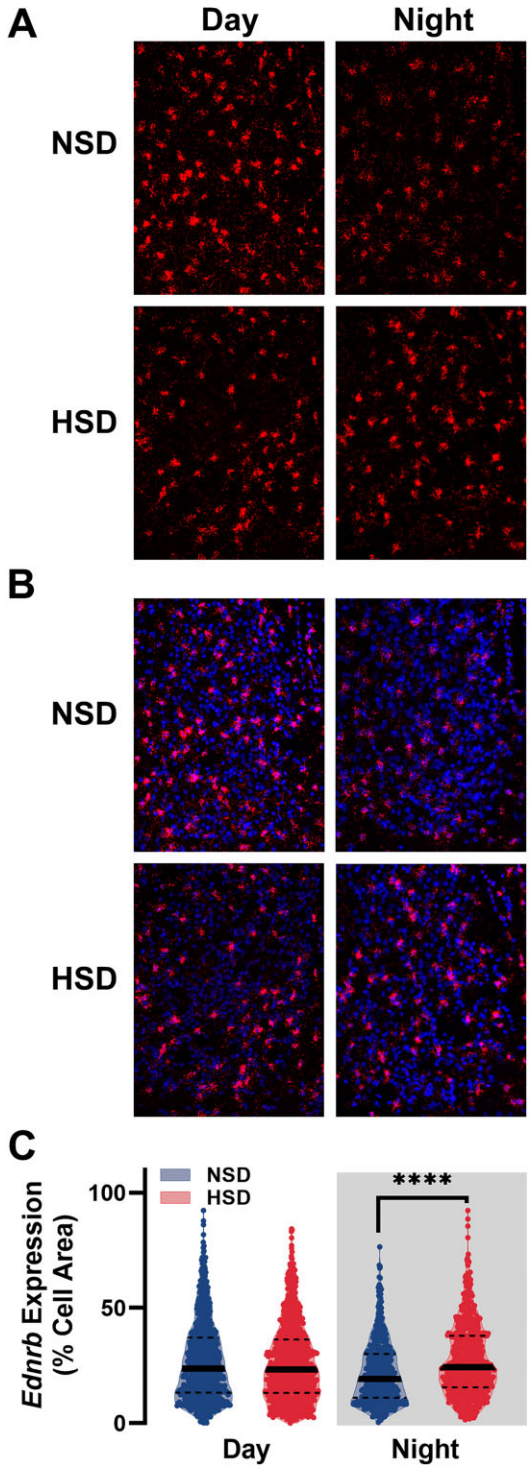

Figure 3. High-salt diet (HSD) increased suprachiasmatic nucleus (SCN) *Ednrb* expression at night. (A and B) Representative fluorescence in situ hybridization (FISH) images of SCN from normal salt diet (NSD) and HSD-fed mice showing expression of *Ednrb* (A) or *Ednrb* (red) plus DAPI (blue, B) expression during the day (Zeitgeber time [ZT] 6) or night (ZT 18). (C) Quantification of *Ednrb* expression per cell from groups represented in A and B. HSD significantly increased expression of *Ednrb* at night (time × diet interaction, $F_{(1974.7)} = 23.209$, $P < .001$; NSD-night vs. HSD-night post hoc, $P < .001$), when *Ednrb* expression is low in NSD-fed mice, but had no effect during the day ($P = .372$). Solid and dotted lines indicate median and quartiles, respectively. $n = 856$ (NSD-day), 931 (HSD-day), 470 (NSD-night), and 657 (HSD-night) cells; 4 (NSD-night) or 6 (NSD-day, HSD-day, and HSD-night) mice per group.

[22.2-24.3]; NSD-day, 24.0% [22.9-25.1]), consistent with the HSD-induced changes in SCN firing rate.

We next sought to confirm the presence of functional ET_B receptors in the SCN and determine whether their activation is sufficient to increase SCN neuronal activity. To do this, we treated acute brain slices from NSD-fed mice with either a selective ET_B agonist (IRL-1620, 10 nM), ET-3 (10 nM), or vehicle (water), and recorded from SCN neurons during the projected night. Both treatments significantly increased SCN firing compared to vehicle-treated controls (median [IQR]: Veh, 0.11 [0.00-2.18]; IRL-1620, 1.26 [0.00-3.11]; ET-3, 1.24 [0.07-3.50 Hz]; Figure 4A and B). Moreover, ET-3-treated cells were 2.93 times more likely to be spiking than vehicle-treated controls (Figure 4C). Together, these results demonstrate that bath application of ET-3 sufficiently mimics the effects of HSD feeding on nighttime SCN excitability.

Given that ET_B receptor activation was capable of increasing SCN firing at night, we next determined whether ET_B receptor activation is necessary for the HSD-induced increase in SCN neuronal activity at night. To do this, we fed mice NSD or HSD for 2 weeks and then recorded from SCN neurons at night in the presence of chronically bath-applied ET_B antagonist (A-1922621, 1 μM) or vehicle control (DMSO, 0.03%). As expected, in vehicle-treated slices, SCN cells from HSD-fed animals had a significantly higher spike rate compared to NSD controls (median [IQR]: NSD-veh, 0.08 [0.00-1.31]; HSD-veh, 2.21 [0.24-4.51 Hz]; Figure 5A and B). Treatment with the ET_B antagonist significantly reduced the spontaneous firing rate of cells from HSD-fed mice but had no effect on cells from NSD-fed animals (median [IQR]: HSD, 0.20 [0.00-2.56]; NSD, 0.00 [0.00-1.29 Hz]). Although the HSD + antagonist cells were still significantly more excitable than NSD + antagonist cells ($P = .018$), neuronal activity was restored to levels similar to the NSD + veh group ($P = .521$). Moreover, the proportion of silent cells were similar across all groups except the HSD + veh, with HSD + veh cells 3.44 times more likely to be spiking than HSD + antagonist cells (Figure 5C). Taken together, these results suggest that local ET_B signaling in the SCN contributes to HSD-induced changes in neuronal excitability.

In other brain areas, ET_B receptors are localized to both neurons and astrocytes[13]; however, a recent single-cell RNA-seq study in the SCN reported a substantial enrichment of *Ednrb* specifically in astrocytes.[12,29] Similarly, we found co-expression of *Ednrb* in cells expressing the astrocytic marker, *Gfap*, but not in cells expressing the neuronal marker, *Eno2* (Supplemental Figure S2), confirming the astrocytic enrichment of *Ednrb* in the SCN. In the SFO, activation of glial ET_B receptors promotes the release of lactate, which can be taken up into neurons through monocarboxylate transporters (MCTs), and leads to increased excitability in local neurons.[14] To test whether lactate was also involved in the SCN neuronal response to ET-3, we performed loose-patch recordings of SCN neurons from NSD-fed animals at night (projected ZT 14-18) in the presence of vehicle (DMSO, 0.2%), ET-3 (10 nM), the MCT inhibitor, CHC (200 μM), or ET-3 + CHC. Consistent with our above findings, ET-3 treatment significantly increased the spike rate of SCN neurons compared to vehicle-treated controls (median [IQR]: veh, 0.01 [0.00-0.80]; ET-3, 1.27 [0.00-3.56 Hz]; Figure 6A and B). Treatment with the MCT blocker, CHC, completely blocked this ET-3-induced excitability (median [IQR]: CHC, 0.02 [0.00-0.71]; ET-3 + CHC, 0.02 [0.00-0.92 Hz]), while CHC had no effect on SCN firing rate in vehicle-treated slices. Furthermore, ET-3-treated slices had a significantly higher percentage of spiking cells compared to all other treatment groups,

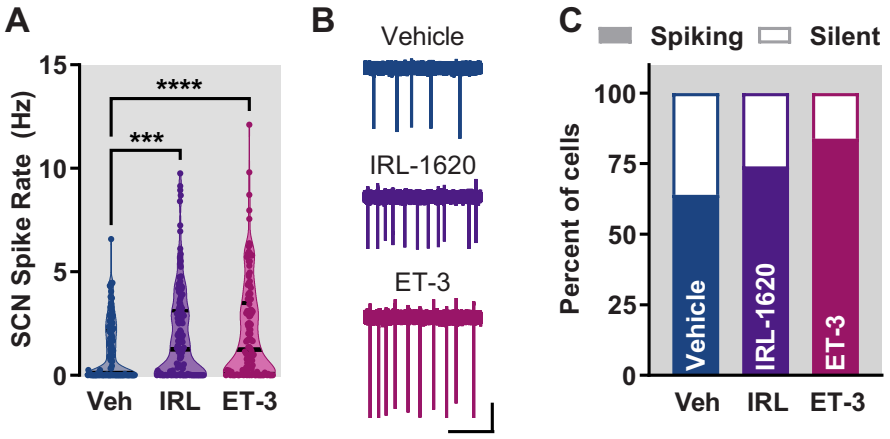

Figure 4. Endothelin B (ET_B) activation increases nighttime suprachiasmatic nucleus (SCN) neuronal activity. (A) Violin plots of spontaneous action potential frequencies of neurons from SCN slices treated with vehicle (water), ET_B agonist (IRL-1620, 10 nM) or ET-3 (10 nM). Both treatments significantly increase spontaneous firing rate compared to vehicle ($H_{(2)} = 17.842$, $P < .001$). Solid and dotted lines indicate median and quartiles, respectively. $n = 133$ (vehicle), 146 (IRL-1620), and 130 (ET-3) cells; 3 mice per group. $^{**}P = .007$, $^{***}P < .001$. (B) Representative loose-patch traces (5 s) from each group. Scale bars: 2 s, 50pA. (C) Percentage of silent (empty bars) versus spiking (filled bars) for cells differed between groups ($\chi^2_{(2)} = 13.529$, $P = .001$), with significantly more silent cells in ET-3-treated slices compared to vehicle ($P < .05$).

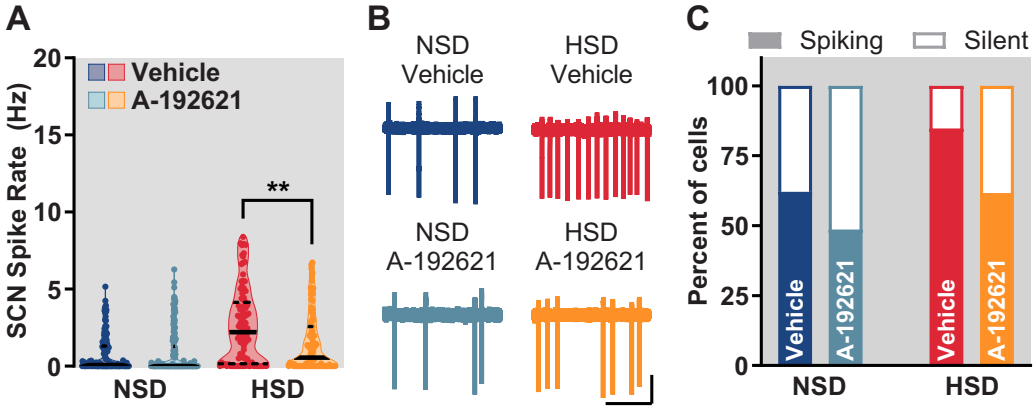

Figure 5. Endothelin B (ET_B) antagonist reduces high-salt diet (HSD)-induced suprachiasmatic nucleus (SCN) hyperexcitability at night. (A) Violin plots of spontaneous action potential frequencies of SCN neurons treated with ET_B antagonist (A-192621, 1 μM) or vehicle (DMSO, 0.03%) from normal salt diet- (NSD-) or HSD-fed mice. Blocking ET_B significantly reduced neuronal activity in neurons from HSD-fed mice (diet × treatment interaction, $H_{(1)} = 9.430$, $P = .002$; HSD-veh vs. HSD-antagonist post hoc, $P < .001$), but did not affect neurons from NSD-fed controls ($P = 1.00$). Solid and dotted lines indicate median and quartiles, respectively. $n = 153$ (NSD-veh), 177 (NSD-antagonist), 176 (HSD-veh), and 172 (HSD-antagonist) cells; 4 mice per group. (B) Representative loose-patch traces (5 s) from each group. Scale bars: 2 s, 50pA. (C) Percentage of silent (empty bars) versus spiking (filled bars) for cells differed between groups (3-way interaction, $\chi^2_{(1)} = 3.965$, $P = .046$), with HSD-veh slices having significantly more spiking cells than all other groups ($P < .05$).

with ET-3-treated cells 2.19 times more likely to be spiking than ET-3 + CHC–treated cells (Figure 6C).

In a nearby hypothalamic region, the supraoptic nucleus (SON), astrocytic ET_B receptor activation has been shown to augment neuronal activity through glutamatergic signaling.[13] Moreover, recent work has demonstrated that glutamate serves as a mechanism by which astrocytes regulate SCN neuronal synchrony.[30] Therefore, we next tested whether glutamatergic signaling underlies the increase in neuronal activity in response to ET-3 in the SCN. To do this, we performed loose-patch recordings from SCN neurons from NSD-fed animals at night (projected ZT 14-18) in the presence of vehicle (water), ET-3 (10 nM), the NMDA blocker, CPP (10 μM), or ET-3 + CPP. Consistent with our above findings, ET-3 treatment significantly increased the spike rate of SCN neurons, compared to vehicle-treated controls (median [IQR]: veh, 0.02 [0.00-0.85]; ET-3, 1.22 [0.05-4.34 Hz]; Figure 7A and B). Remarkably, treatment with the NMDA antagonist, CPP, completely blocked this ET-3-induced excitability (median [IQR]: CPP, 0.08 [0.00-1.25]; ET-3 + CPP, 0.07 [0.00-1.08 Hz]). In the presence of vehicle, CPP had no effect on SCN firing rate. Similar to the effect on spike rate, ET-3-treated slices had a significantly lower percentage of silent cells, compared to all other treatment groups, with ET-3-treated cells 3.9 times more likely to be spiking than ET-3 + CPP–treated cells (Figure 7C). Together, these results suggest that glutamatergic signaling mediates the excitatory effects of ET-3 on SCN neurons at night.

Discussion

The goal of our current study was to determine the impact of high salt intake on output signaling of the central circadian pacemaker, as well as explore the ET system as a possible mechanism underlying these changes. Here, we present 3 major findings: (1) 2 weeks of HSD feeding is sufficient to change the organization of daily wheel running without impacting the overall activity levels, (2) chronic HSD enhances SCN neuronal excitability at night due to local ET signaling involving activation of ET_B receptors localized to SCN astrocytes, and (3) ET-3-driven neuronal activation depends on MCT function and NMDA receptor activation. To our knowledge, our results are the first to

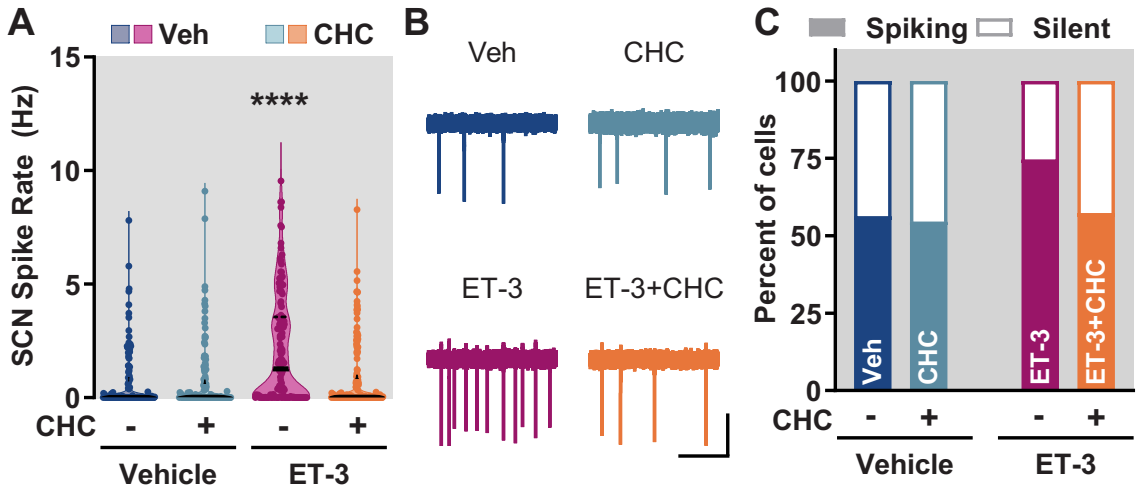

Figure 6. Suprachiasmatic nucleus (SCN) neuronal response to endothelin-3 (ET-3) is dependent on monocarboxylate transporter (MCT) lactate transporters. (A) Violin plots of spontaneous action potential frequencies of neurons from SCN slices treated with vehicle (DMSO, 0.2%), MCT inhibitor (2-cyano-3-(4-hydroxyphenyl)-2-propenoic acid [CHC], 200 μM), ET-3 (10 nM), or CHC + ET-3. ET-3 significantly increased SCN firing rate, and this was blocked with CHC (CHC × ET-3 interaction, $H_{(1)} = 12.70$, $P < .001$). Solid and dotted lines indicate median and quartiles, respectively. $n = 135$ (veh), 130 (CHC), 134 (ET-3), and 143 (CHC + ET-3) cells; 3 mice per group. ****$P < .001$ compared to all other groups. (B) Representative loose-patch traces (5 s) from each group. Scale bars: 2 s, 50pA. (C) Percentage of silent (empty bars) versus spiking (filled bars) for cells differed between treatment groups (3-way interaction, $\chi^2_{(1)} = 3.971$, $P = .046$), with ET-3 slices having significantly more spiking cells than all other groups ($P < .05$).

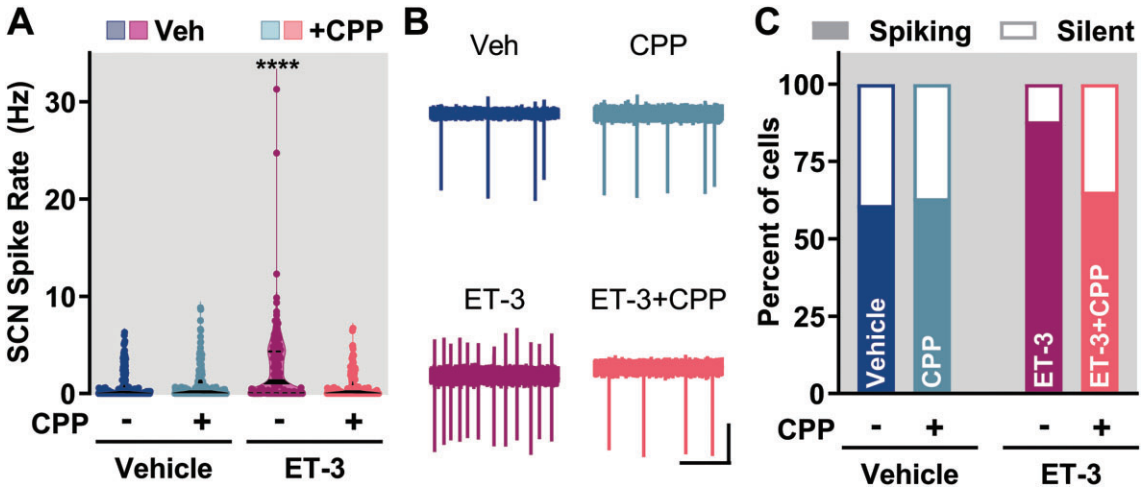

Figure 7. NMDA receptors mediate suprachiasmatic nucleus (SCN) neuronal response to endothelin-3 (ET-3). (A) Violin plots of spontaneous action potential frequencies of neurons from SCN slices treated with vehicle (water), NMDA blocker (3-(2-carboxyp-iperazin-4-yl)propyl-1-phosphonic acid [CPP], 10 μM), ET-3 (10 nM), or CPP + ET-3. ET-3 significantly increased SCN firing rate, and this was blocked with CPP (CPP × ET-3 interaction, $H_{(1)} = 30.018$, $P < .001$). Solid and dotted lines indicate median and quartiles, respectively. $n = 192$ (veh), 195 (CPP), 183 (ET-3), and 187 (CPP + ET-3) cells; 4 mice per group. ****$P < .001$ compared to all other groups. (B) Representative loose-patch traces (5 s) from each group. Scale bars: 2 s, 50pA. (C) Percentage of silent (empty bars) versus spiking (filled bars) for cells differed between treatment groups (3-way interaction, $\chi^2_{(1)} = 18.157$, $P < .001$), with ET-3 slices having significantly more spiking cells than all other groups ($P < .05$).

demonstrate a novel mechanism for the circadian effects of HSD mediated by the ET-3 peptide that appears to be derived from endothelial cells to activate ET_B receptors in the SCN including a novel role for SCN astrocytes.

Our initial finding that HSD feeding disrupts typical circadian behavior contributes to the growing body of literature highlighting the SCN as a mediator of fluid-electrolyte control. A recent study reported that increases in late-night neuronal activity in arginine vasopressin-expressing SCN neurons projecting to the OVLT were responsible for an increase in water intake during the end of the active phase.[7] C57BL6 mice exhibit a distinct pattern of nocturnal behavior with 2 distinct bouts of activity separated by a period of sleep often referred to as the "siesta."[22,23,31] In this study, we found that 2 weeks of HSD led to a reorganization of nighttime activity such that the initial activity bout was extended into the mid-to-late night "siesta" period. This resulted in a shortened second bout of activity, with the second bout of activity entirely lost in half of the HSD-fed animals. These changes in locomotor activity coincided with an increase in SCN neuronal activity in the early-mid night (ZT 14-18). Although future experiments are needed to determine the physiological changes driving this reorganization of nighttime activity, it is possible that this increase in SCN firing extends the active phase in order to lengthen the period of drinking (offsetting the high salt intake). While we do not measure water intake in this study, this theory is consistent with our previous work showing increased water intake in HSD-fed rats[25] and mice,[32] primarily during the active (ie, dark) phase. Future experiments

examining fluid intake at a higher resolution are needed to fully elucidate the timing of these changes. Interestingly, in humans, sodium intake has been reported to have an opposite effect on water consumption in the long term.[33] Given that SCN activity rhythms appear to be similar in both nocturnal and diurnal mammals, with higher activity in the light phase,[34] further research into SCN control of thirst could provide valuable insight into how these dynamics change across temporal niche.

Our finding that HSD-induced neuronal excitability is driven by local endothelin signaling is supported by multiple pieces of evidence. First, we demonstrate that endothelial cells within the SCN express *Edn3*, the gene encoding ET-3, consistent with a previous single-cell RNA-sequencing study.[12] Second, the increase in SCN spike rate persists for up to 6 h after external influences have been removed. Moreover, acute treatment with an ET_B antagonist reverses the effects of HSD ex vivo. Although this evidence supports a model with local SCN endothelial cell release of ET-3, it is important to note that circulating ETs in the blood or surrounding brain regions could also contribute to the behavioral effects of HSD. Thus, future research should investigate the signaling mechanisms of dietary sodium to SCN endothelial cells, the length of time that the effects of HSD persist after diet reversal, and the identification of other rhythmic processes in the SCN that are impacted by HSD. Prior single-cell RNA-sequencing study of the SCN did not reveal detectable expression of ET-1 (*Edn1*)[12] that is considered the primary endothelial-derived isoform. Consistent with these findings, we were unable to detect ET-1 expression in the SCN using in situ hybridization (data not shown).

Although this study demonstrated a role for ET signaling in the SCN response to HSD, more work is needed to determine the functional role of ET in central circadian regulation under normal, unchallenged, conditions. Recent work has demonstrated the existence of the portal vein system in which blood flows from the SCN to the nearby OVLT at a higher rate at night than during the day, driven by an as yet undetermined mechanism.[35] Interestingly, the rhythmic expression of *Edn3* in SCN endothelial cells also peaks during the early night phase,[12] which raises the possibility for ET-3 contributing to the changes in flow rate across time of day. Given that HSD-fed animals had an increase in *Ednrb* expression at night, when *Edn3* is reportedly higher, it is possible that an increase in ET_B receptors sensitizes the SCN to a normally occurring nightly increase in ET-3 release. However, a limitation of this study is the lack of measurement of ET-3 release in the SCN in response to HSD. Thus, we cannot rule out the possibility that a change in ET-3 release also contributes to the HSD-induced excitability in the SCN. In fact, previous work has demonstrated an increase in ET-3 release in the SFO following dehydration,[14] so future research should examine whether a similar process occurs within the SCN in response to HSD.

Although ET_B receptors have been found to be present on both astrocytes and neurons in other brain regions,[9,13] our data suggest these receptors are restricted to astrocytes alone in the SCN. This is consistent with recent single-cell RNA sequencing data showing *Ednrb* as an astrocytic marker in the SCN.[12] Additionally, we found that ET-3-induced excitability was dependent on MCTs, which allow for the transport of lactate from astrocytes to neurons,[36] consistent with previous findings in the SFO.[14] As regulators of the blood-brain barrier, astrocytes are perfectly positioned to serve as a mediator between circulating signals and neurons. In fact, even in a brain region with both astrocytic and neuronal expression of ET_B receptors, like the SON, the neuronal response to ET_B signaling appears to be indirect. Specifically, ET_B-induced changes in neuronal activity were dependent on astrocytic modulation of glutamate or nitric oxide for excitatory or inhibitory responses, respectively.[13] The present results show that ET-3 excited SCN neurons at night, and thus, we focused on glutamate-mediated signaling and found that this excitatory effect was dependent upon NMDA receptor activation. However, future work should examine the possible mechanisms by which astrocytic ET_B activation may augment glutamatergic signaling, such as Ca^{2+}-dependent exocytosis or modulation of excitatory amino acid transporters.[36] In fact, previous work has shown that neuronal lactate uptake can lead to potentiation of NMDA receptors through alteration of redox state.[37] Given that extracellular levels of glutamate are already elevated in the SCN at night,[30] lactate-driven changes in NMDA receptor sensitivity could provide a mechanism for ET-3-induced excitability without a need for additional glutamate release. Interestingly, astrocytic regulation of daily rhythms in extracellular glutamate has recently been shown to contribute to SCN network synchrony.[30] Therefore, future work should examine the impact of HSD consumption and/or endothelin signaling on intra-SCN coupling as well.

Author Contributions

Jodi R. Paul (Conceptualization, Data curation, Formal analysis, Investigation, Methodology, Validation, Visualization, Writing—original draft, Writing—review & editing), Megan K. Rhoads (Conceptualization, Data curation, Formal analysis, Methodology, Visualization, Writing—review & editing), Anna Elam (Data curation), David M. Pollock (Conceptualization, Formal analysis, Funding acquisition, Investigation, Resources, Software, Supervision, Visualization, Writing—original draft, Writing—review & editing), and Karen L. Gamble (Conceptualization, Data curation, Formal analysis, Funding acquisition, Investigation, Methodology, Project administration, Resources, Supervision, Visualization, Writing—review & editing)

Supplementary Material

Supplementary material is available at the *APS Function* online.

Funding

National Institute of Diabetes and Digestive and Kidney Diseases: R01 DK134562 (to D.M.P. and K.L.G.); American Heart Association Postdoctoral Fellowship: 827566 (to M.K.R.); and American Heart Association Career Development Award: 24CDA1046338 (to M.K.R.).

Conflict of Interest Statement

D.M.P. holds the position of Editor-in-Chief for *FUNCTION* and is blinded from reviewing or making decisions for the manuscript. K.L.G. holds the position of Editorial Board Member for *FUNCTION* and is blinded from reviewing or making decisions for the manuscript.

Data Availability

Source data are available at 10.6084/m9.figshare.28525553.

References

1. Rosenwasser AM, Turek FW. Neurobiology of circadian rhythm regulation. *Sleep Med Clin* 2015;**10**(4):403–412.
2. Douma LG, Barral D, Gumz ML. Interplay of the circadian clock and endothelin system. *Physiology* 2021;**36**(1):35–43.
3. Takahashi JS. Molecular components of the circadian clock in mammals. *Diabetes Obes Metab* 2015;**17**(S1):6–11.
4. Paul JR, Davis JA, Goode LK, et al. Circadian regulation of membrane physiology in neural oscillators throughout the brain. *Eur J Neurosci* 2020;**51**(1):109–138.
5. Gizowski C, Bourque CW. Sodium regulates clock time and output via an excitatory GABAergic pathway. *Nature* 2020;**583**(7816):421–424.
6. Zimmerman CA. The origins of thirst. *Science* 2020;**370**(6512):45–46.
7. Gizowski C, Zaelzer C, Bourque CW. Clock-driven vasopressin neurotransmission mediates anticipatory thirst prior to sleep. *Nature* 2016;**537**(7622):685–688.
8. Davenport AP, Hyndman KA, Dhaun N, et al. Endothelin. *Pharmacol Rev* 2016;**68**(2):357–418.
9. Kohan DE, Rossi NF, Inscho EW, Pollock DM. Regulation of blood pressure and salt homeostasis by endothelin. *Physiol Rev* 2011;**91**(1):1–77.
10. Jin C, Speed JS, Pollock DM. High salt intake increases endothelin B receptor function in the renal medulla of rats. *Life Sci* 2016;**159**:144–147.
11. Soliman RH, Pollock DM. Circadian control of sodium and blood pressure regulation. *Am J Hypertens* 2021;**34**(11):1130–1142.
12. Wen S, Ma D, Zhao M, et al. Spatiotemporal single-cell analysis of gene expression in the mouse suprachiasmatic nucleus. *Nat Neurosci* 2020;**23**(3):456–467.
13. Filosa JA, Naskar K, Perfume G, et al. Endothelin-mediated calcium responses in supraoptic nucleus astrocytes influence magnocellular neurosecretory firing activity. *J Neuroendocrinol* 2012;**24**(2):378–392.
14. Hiyama TY, Yoshida M, Matsumoto M, et al. Endothelin-3 expression in the subfornical organ enhances the sensitivity of Na(x), the brain sodium-level sensor, to suppress salt intake. *Cell Metab* 2013;**17**(4):507–519.
15. Becker BK, Grady CM, Markl AE, Torres Rodriguez AA, Pollock DM. Elevated renal afferent nerve activity in a rat model of endothelin B receptor deficiency. *Am J Physiol Renal Physiol* 2023;**325**(2):F235–F247.
16. Heimlich JB, Speed JS, Bloom CJ, O'Connor PM, Pollock JS, Pollock DM. ET-1 increases reactive oxygen species following hypoxia and high-salt diet in the mouse glomerulus. *Acta Physiologica* 2015;**213**(3):722–730.
17. Molina PA, Edell CJ, Dunaway LS, et al. Aryl hydrocarbon receptor activation promotes effector CD4+ T cell homeostasis and restrains salt-sensitive hypertension. *Function (Oxf)* 2025. https://doi.org/10.1093/function/zqaf001.
18. Shimada S, Hoffmann BR, Yang C, et al. Metabolic responses of normal rat kidneys to a high salt intake. *Function (Oxf)* 2023;**4**(5):zqad031.
19. Pastrick A, Diaz M, Adaya G, et al. Biological sex influences daily locomotor rhythms in mice held under different housing conditions. *J Biol Rhythms* 2024;**39**(4):351–364.
20. Alvord VM, Pendergast JS. The estrous cycle coordinates the circadian rhythm of eating behavior in mice. *J Biol Rhythms* 2024;**39**(5):413–422.
21. Paul JR, Johnson RL, Jope RS, Gamble KL. Disruption of circadian rhythmicity and suprachiasmatic action potential frequency in a mouse model with constitutive activation of glycogen synthase kinase 3. *Neuroscience* 2012;**226**:1–9.
22. Collins B, Pierre-Ferrer S, Muheim C, et al. Circadian VIPergic neurons of the suprachiasmatic nuclei sculpt the sleep-wake cycle. *Neuron* 2020;**108**(3):486–499.e5.
23. Ehlen JC, Jones KA, Pinckney L, et al. Maternal Ube3a loss disrupts sleep homeostasis but leaves circadian rhythmicity largely intact. *J. Neurosci.* 2015;**35**(40):13587–13598.
24. Paul JR, DeWoskin D, McMeekin LJ, Cowell RM, Forger DB, Gamble KL. Regulation of persistent sodium currents by glycogen synthase kinase 3 encodes daily rhythms of neuronal excitability. *Nat Commun* 2016;**7**:(1):13470.
25. Rhoads MK, Speed JS, Roth KJ, et al. Short-term daytime restricted feeding in rats with high salt impairs diurnal variation of Na(+) excretion. *Am J Physiol Renal Physiol* 2022;**322**(3):F335–F343.
26. Xiao H, Lu H, Xue Y, et al. Deleterious effect in endothelin receptor-mediated coronary artery smooth muscle contractility in high-salt diet rats. *Nutr Metab Cardiovasc Dis* 2023;**33**(1):234–244.
27. Tsai YH, Ohkita M, Gariepy CE. Chronic high-sodium diet increases aortic wall endothelin-1 expression in a blood pressure-independent fashion in rats. *Exp Biol Med (Maywood)* 2006;**231**(6):813–817.
28. Iwasa N, Emoto N, Widyantoro B, Miyagawa K, Nakayama K, Hirata K. Knockout of endothelin-1 in vascular endothelial cells protects against insulin resistance induced by high-salt diet in mice. *Kobe J Med Sci* 2010;**56**(2):E85–E91. .
29. Morris EL, Patton AP, Chesham JE, Crisp A, Adamson A, Hastings MH. Single-cell transcriptomics of suprachiasmatic nuclei reveal a Prokineticin-driven circadian network. *EMBO J* 2021;**40**(20):e108614.
30. Brancaccio M, Patton AP, Chesham JE, Maywood ES, Hastings MH. Astrocytes control circadian timekeeping in the suprachiasmatic nucleus via glutamatergic signaling. *Neuron* 2017;**93**(6):1420–1435.e5.
31. Whitney MS, Shemery AM, Yaw AM, Donovan LJ, Glass JD, Deneris ES. Adult brain serotonin deficiency causes hyperactivity, circadian disruption, and elimination of siestas. *J Neurosci.* 2016;**36**(38):9828–9842.
32. Zhang D, Jin C, Obi IE, et al. Loss of circadian gene Bmal1 in the collecting duct lowers blood pressure in male, but not female, mice. *Am J Physiol Renal Physiol* 2020;**318**(3):F710–F719.
33. Rakova N, Kitada K, Lerchl K, et al. Increased salt consumption induces body water conservation and decreases fluid intake. *J Clin Invest* 2017;**127**(5):1932–1943.
34. Bano-Otalora B, Moye MJ, Brown T, Lucas RJ, Diekman CO, Belle MD. Daily electrical activity in the master circadian clock of a diurnal mammal. *eLife* 2021;**10**:e68179. doi: 10.7554/eLife.68179.
35. Roy RK, Yao Y, Green IK, et al. Blood flows from the SCN toward the OVLT within a new brain vascular portal pathway. *Sci. Adv.* 2024;**10**(25):eadn8350.
36. Malarkey EB, Parpura V. Mechanisms of glutamate release from astrocytes. *Neurochem Int* 2008;**52**(1–2):142–154.
37. Jourdain P, Rothenfusser K, Ben-Adiba C, Allaman I, Marquet P, Magistretti PJ. Dual action of L-Lactate on the activity of NR2B-containing NMDA receptors: from potentiation to neuroprotection. *Sci Rep* 2018;**8**(1):13472.

Submitted: 24 December 2024; **Revised:** 12 February 2025; **Accepted:** 2 March 2025